Neural Surface Priors for Editable Gaussian Splatting

Jakub Szymkowiak[*1,2,†]   Weronika Jakubowska[*3,‡]   Dawid Malarz[1,4]   Weronika Smolak-Dyżewska[1,4]

Maciej Zięba[3,5]   Wojtek Pałubicki[2]   Przemysław Musialski[1,6]   Przemysław Spurek[1,4]

[1]IDEAS NCBR   [2]Adam Mickiewicz University   [3]Wrocław University of Science and Technology

[4]Jagiellonian University   [5]Tooploox   [6]New Jersey Institute of Technology

[†]jakub.szymkowiak@ideas-ncbr.pl, [‡]weronika.jakubowska@pwr.edu.pl

[*]Equal contribution

Extracted Mesh   **Recovered Appearance**   **Proxy Representation**   **Modified Mesh**   **Final Result**
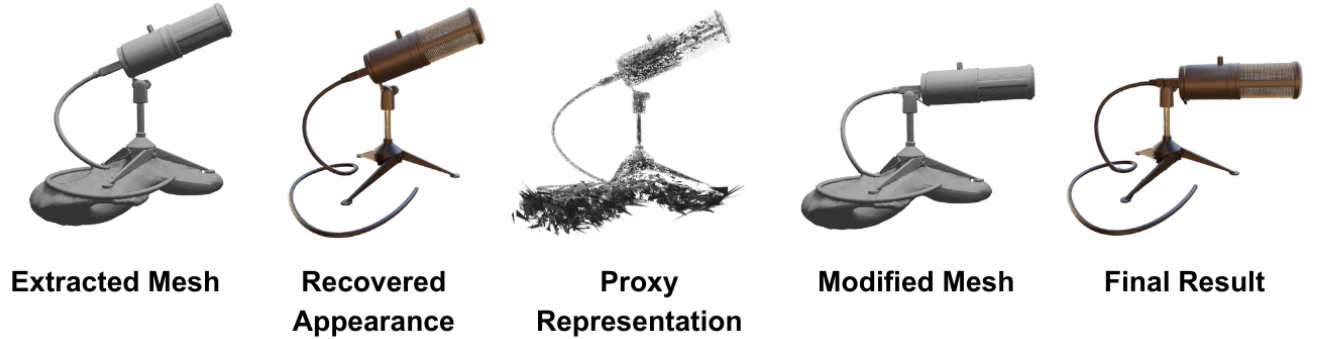
Figure 1. We propose a new method for deriving an editable, 3DGS-based appearance representation of the scene from a set of input images. We're employing a pretrained neural surface prior, which allows us to extract a high-quality mesh. Modifications to the mesh geometry propagate to the recovered appearance, allowing for easy and intuitive editing of the represented objects with high visual fidelity.

Abstract

In computer graphics, there is a need to recover easily modifiable representations of 3D geometry and appearance from image data. We introduce a novel method for this task using 3D Gaussian Splatting, which enables intuitive scene editing through mesh adjustments. Starting with input images and camera poses, we reconstruct the underlying geometry using a neural Signed Distance Field and extract a high-quality mesh. Our model then estimates a set of Gaussians, where each component is flat, and the opacity is conditioned on the recovered neural surface. To facilitate editing, we produce a proxy representation that encodes information about the Gaussians' shape and position. Unlike other methods, our pipeline allows modifications applied to the extracted mesh to be propagated to the proxy representation, from which we recover the updated parameters of the Gaussians. This effectively transfers the mesh edits back to the recovered appearance representation. By leveraging mesh-guided transformations, our approach simplifies 3D scene editing and offers improvements over existing methods in terms of usability and visual fidelity of edits. The complete source code for this project can be accessed at https://github.com/WJakubowska/NeuralSurfacePriors

1. Introduction

Recovering scene appearance has long been a task in computer graphics. Recently, 3D Gaussian Splatting (3DGS) [8] has gained significant attention for its fast training times and real-time viewing capabilities. Neural Radiance Fields (NeRF) [12] and similar methods [2, 14, 28] query neural networks, parametric grids, or a hybrid of those two, to sample color density along each ray. In contrast, 3DGS

arXiv:2411.18311v1 [cs.CV] 27 Nov 2024

eliminates the need for volumetric rendering altogether and replaces it with a set of optimizable Gaussian kernels and a Gaussian rasterizer which drastically improves learning and inference times. To capture the scene appearance, 3DGS independently optimizes a number of parameters (position in world space, scaling, rotation, and coefficients of spherical harmonics) of each Gaussian kernel, producing a mixture of many thousands of local appearance estimators.

However, neither 3DGS or NeRF recover a connected surface mesh of the scene or allow for convenient modifications of the recovered scene geometry, both important in many applications. Recovering a mesh geometry has the advantage that it enables editing of the reconstructed scenes with an array of tools commonly found in computer graphics applications, such as translate, rotate, extrude or subdivision tools. In that case, the modifications made to the mesh have to be propagated to the recovered appearance or else it would not be consistent with the mesh after the editing.

A number of previous work has extended 3DGS for the task of mesh extraction and scene editing. One approach involves estimating a coarse mesh and binding Gaussians to its surface via an optimization process [7]. In this way, modifications of the mesh can be propagated to the Gaussians for consistent appearance. Often, mesh extraction involves jointly training a neural signed distance field (SDF) and applying the Marching Cubes [10, 15] algorithm to obtain a mesh, but this does not recover the color appearance of objects. Other works [23] propose to skip the mesh extraction part, and modify the Gaussian kernels using a proxy representation, such as a triangle soup. Changes in the proxy representation affect the geometry of the Gaussians, resulting in modifications to the recovered appearance. While this approach does not require additional geometry estimation (such as a mesh), using a triangle soup proxy is less suitable for editing with existing geometry modification pipelines. This is due to the lack of topology in the triangle soup which limits the use and scope of established computer graphics editing tools.

In this paper, we aim to enable joint editing of mesh and Gaussians by loosely aligning the 3D Gaussians with a neural surface prior making an additional optimization step as used in other methods (e.g. [7]) unnecessary. This approach allows us to use a high-quality mesh for editing operations, and propagate the modifications made to its geometry directly to the proxy representation, and hence to the recovered appearance via matrix transformations. Due to the access to high-quality meshes in our prior-based approach we facilitate the use of physical simulations on recovered objects, as many numerical methods require detailed mesh geometries (e.g. finite element methods). Specifically, our novel method uses flat Gaussian components, and conditions their opacity on the distance from the object, to facilitate close alignment with the surface geometry, but does

not directly bind them to it. Then, by utilizing a shortest distance correspondence between our triangle soup proxy representation and the extracted mesh, any changes made to the mesh geometry are reflected in a modification of the proxy.

In summary, our contributions are as follows:
- We introduce a novel method for geometry and appearance recovery from image data, suitable for mesh-guided editing.
- We show that our approach allows for easy manual modification of the scene, achieving high visual quality.
- We include an experiments section, where we test our approach for appearance recovery, geometry-based editing, and physical simulations.

2. Related Work

Recent advancements in computer graphics and vision have significantly enhanced our ability to recover and manipulate scene appearances. In this section, we provided a brief overview of the developments in the field, focusing on techniques that build upon 3D Gaussian Splatting for geometry recovery and scene modification.

Novel view synthesis. Novel view synthesis is a task of generating images of the scene from unseen viewpoints based on a collection of ground truth views. Neural rendering methods, such as NeRF [12], have leveraged deep learning methods to surpass the traditional Structure from Motion [16, 20] and Multi-View Stereo [6] pipelines in terms of the visual fidelity of the reconstructed scenes. These techniques employ volumetric rendering, originally introduced in [4], to sample densities along each ray originating from the viewpoint. While NeRF produces impressive results, the necessity to consider a vast amount of rays results in long training times and costly inference. More recent works have alleviated these issues to a significant extend. Notably, InstantNGP [14] has introduced introduced a differentiable hash-table encoding that allows for rapid training of the NeRF models.

In contrast to volumetric rendering-based methods, 3DGS [8] is a point cloud based technique that models the scene appearance with many thousands of optimizable 3D Gaussian kernels, parametrized by their locations, orientation in space, and colors derived from spherical harmonics. These kernels are then rasterized using a Gaussian kernel rasterizer. This approach not only simplifies the rendering pipeline, but also significantly enhances training and inference efficiency, making it particularly suitable for real-time applications.

Geometry extraction. A number of methods has been proposed to enhance both NeRF [19, 24, 25, 27] and 3DGS

[3, 7, 11] to recover the underlying geometry of the scene in addition to appearance. A popular technique is to condition the opacity on the distance from the surface [11, 24] - high opacity values should align with the represented object's geometry, as it primarily contributes to rendering, while the empty space does not. This approach usually involves jointly a neural network representing a signed distance field (a neural SDF) in addition to the appearance model. Afterwards, a mesh representation of the geometry can be extracted using the Marching Cubes algorithm.

In particular, PermutoSDF [19], uses a dual architecture of two neural networks, where the color network is provided with the geometric information from the SDF network, to produce high-quality representations of the geometry and appearance. 3DGSR [11] extends 3DGS by conditioning the Gaussian kernels opacity on a jointly trained SDF with an additional volumetric rendering regularization. An alternative approach is taken by SuGaR [7] and BakedSDF [27], where the appearance model is strictly bound to a coarse mesh obtained in the first training stage, which is then optimized in further training to recover finer details.

Scene editing. Editing and animation of recovered appearance is essential for producing interactive and customizable environments and capturing complex dynamic phenomena. Modifications to both NeRF [17, 18] and 3DGS [7, 22, 23] has been proposed to allow for scene editing and animating, with 3DGS being especially suited for this task due to its geometric property of representing the underlying geometry as a point cloud of Gaussian kernels.

As there already exists a vast amount of highly-developed tools allowing for editing, animating, and simulating physical interactions that target mesh geometry representations, the task of enhancing the recovered appearance with dynamical effects is inherently linked with geometry extraction. By binding appearance representation to an extracted mesh, SuGaR [7] allows to propagate edits in mesh geometry to changes in appearance. Alternatively, methods such as GaMeS [23] and D-MiSo [22] rely on a proxy representation that encodes the recovered orientations and positions of the Gaussian components in a triangle soup proxy.

While we rely on a proxy triangle soup representation, our method uses a neural surface prior to closely align the appearance with the extracted mesh geometry, and then propagates any edits made to the mesh to the proxy, effectively altering the recovered appearance of the scene. It thus allows for easy, mesh-guided scene modifications without explicitly binding the appearance to the geometry.

3. Method

Given a dataset of images and camera poses, our goal is to recover the appearance of an object using our 3DGS-based pipeline, which is designed to enable scene modification
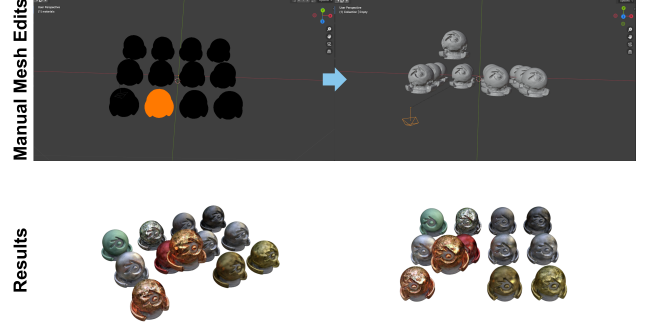

Figure 2. Unlike previous methods utilizing a triangle soup proxy, our approach enables easy modifications of the recovered appearance by editing the underlying mesh (e.g. selecting sub-components and translating them) using any geometry sculpting software, such as as Blender.

through adjustments to an underlying mesh structure. Our pipeline takes comprises three main stages:

1. First, we use PermutoSDF [19] to obtain a neural SDF model that guides the opacity of Gaussian kernels and enables mesh extraction with Marching Cubes for future editing.
2. Second, we train a 3DGS-based model to recover the appearance from image data. In our method, we condition the opacity of the Gaussian kernels based on their distance from the neural surface and ensure each Gaussian lies flat on the surface by fixing one scaling parameter to a small value. Additionally, we incorporate a regularizer that aims to align Gaussian kernels' normals with the normals predicted by the SDF prior.
3. Third, we encode the shapes and positions of each Gaussian into a triangle soup proxy. We associate each triangle in the proxy with the nearest face of the extracted mesh, and manually adjust the mesh by editing it in a geometry sculpting or animation software. Given the correspondence between the original mesh faces, and faces from the manually modified mesh, we are able to propagate the modification to the triangle soup proxy. Finally, we recover updated positions and orientations of the Gaussians, thereby altering the recovered appearance of the scene.

The whole pipeline is visualized in Figure 3. The following sections explain each consecutive stage in more detail.

Obtaining the neural surface prior. Our method starts with a collection of images representing a scene from multiple viewpoints and a set of associated camera poses. In the first stage, we aim to obtain a surface prior in the form of a neural network $f_\theta \colon \mathbf{R}^3 \to \mathbf{R}$ representing the signed distance to the object. This is a crucial step as this neural
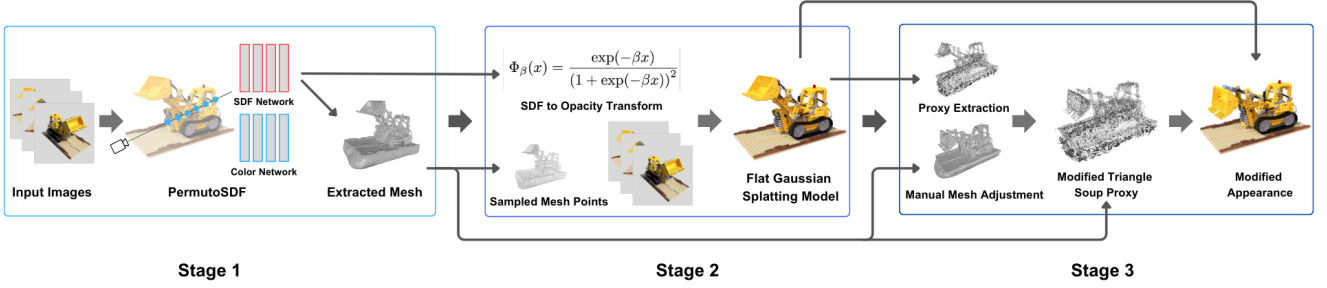
Figure 3. Schematic overview of the pipeline employed by our method. (1) Starting with a collection of input images and corresponding camera poses, the initial stage utilizes PermutoSDF to generate a neural SDF and extract a mesh. (2) The second stage involves training a Gaussian Splatting model. The initial locations of kernels are sampled directly from mesh, and the opacity is defined by the minimum distance from the surface. (3) Given the modified mesh, the third stage involves the extraction of a proxy triangle soup representation, which allows for the propagation of the geometric changes onto this proxy. By recovering the updated Gaussian parameters from this modified proxy, a revised appearance representation is obtained.

surface forms a foundation for subsequent stages. While other works propose to jointly train a neural SDF in addition to the appearance model [3, 11], we opted to segregate it into a separate preprocessing stage, as it leads to a more detailed reconstruction of the geometry, and thus enhances the overall fidelity of later appearance modifications.

In particular, for this task we leverage PermutoSDF [19]. The PermutoSDF pipeline is comprised of two small multi-layer perceptrons learning to approximate the signed distance to the object and the view-dependent colors, respectively. Moreover, the color network uses as one of its inputs an additional geometric feature returned by the SDF network. Subsequently, volumetric rendering is applied to generate the images. The crucial strength of PermutoSDF lies in the multi-resolution tetrahedral lattice it employs to encode sampled rays. This acceleration data structure is similar to the hash-tables used in InstantNGP [14]; however, unlike hyper-cubical grids, the number of lattice vertices scales linearly with dimensionality. Consequently it improves training times, and provides the ability to efficiently represent spatio-temporal appearance and geometry.

Recovering the appearance. The goal of the second stage is to produce a Gaussian Splatting model of the recovered appearance suitable for mesh-guided editing. 3D Gaussian Splatting [8] uses input image data and a point cloud obtained using SfM [20] to produce an appearance representation comprised of many thousands of Gaussian kernels. Each individual component is parametrized by a location vector $\mathbf{m} \in \mathbf{R}^3$, opacity value $\sigma \in [0, 1]$, spherical harmonics colors, and a covariance matrix $\boldsymbol{\Sigma}$, which is decomposed as

$$\boldsymbol{\Sigma} = \mathbf{R}\mathbf{S}\mathbf{S}^\top\mathbf{R} \,,$$

where $\mathbf{S}$ is a diagonal scaling matrix, and $\mathbf{R}$ is a rotation matrix. In practice, 3DGS optimizes a vector $\mathbf{s} \in \mathbf{R}^3$ such

that $\mathbf{S} = \mathrm{diag}(\mathbf{s})$, and a quaternion $\mathbf{q}$ representing the rotation $\mathbf{R}$. Each Gaussian component is then rendered using a Gaussian rasterizer to produce novel views of the scene. Importantly, the number of Gaussians in the model adaptively changes during training, splitting or removing individual components based on their contribution to rendering the images.

For our purpose of mesh-guided scene editing, we aim to place each Gaussian component as aligned with the neural surface prior obtained in the first stage as possible. To this end, we modify the model described above in the following ways. Start by denoting the neural network representing the recovered surface by f_θ. In our model, the opacity is not a learnable parameter, and instead is conditioned on the distance from the surface. More precisely, for each component, the opacity is a function of $f_\theta(\mathbf{x})$, where $\mathbf{x}$ denotes the location of the center. Formally, $\sigma(\mathbf{x}) = (\Phi_\beta \circ f_\theta)(\mathbf{x})$, where

$$\Phi_\beta(x) = \frac{\exp(-\beta x)}{\left(1 + \exp(-\beta x)\right)^2} \,,$$

with β being a learnable parameter, is a bell-shaped function adopted from 3DGSR [11]. Intuitively, the higher the value of β, the better the alignment with the surface, although β being too large leads to numerical instabilities.

Following GaMeS [23], we optimize two of the three scaling factors for each Gaussian, while fixing one to a negligible value of $\varepsilon = 10^{-8}$. This results in Gaussians being essentially two dimensional or flat. Moreover, we incorporate the following regularizer to encourage the optimized normal direction of each Gaussian kernel to align with the normal predicted by the SDF:

$$\mathcal{L}_{\mathrm{normal}}(\mathbf{x}) = \left| 1 - |\mathbf{n}(\mathbf{x})^\top \nabla f_\theta(\mathbf{x})| \right| \,.$$

Here, $\mathbf{x}$ denotes the center of a single Gaussian, and $\mathbf{n}(\mathbf{x})$ is the corresponding normal, which in our case is the first col-
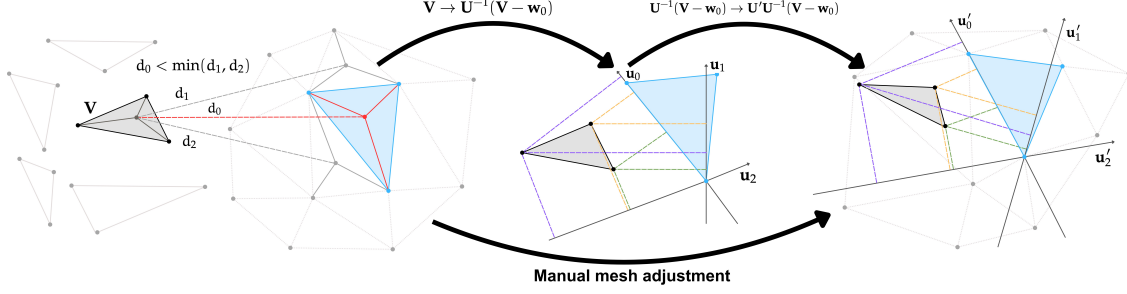
4

Figure 4. Visualization of propagating the mesh edit to a single proxy triangle. We start by connecting the triangle $\mathbf{V}$ to the nearest mesh face (pictured in light blue). Then, its coordinates are expressed in the associated basis $\mathbf{U}$ (represented in the picture by gray axes pointing in the directions given by the basis). A subsequent transformation aligns the triangle in the modified basis $\mathbf{U}'$, resulting in an updated representation of a single Gaussian's shape and position.

umn of the rotation matrix. The rest of the pipeline remains the same as in 3DGS.

Mesh-guided appearance modification. In the third stage, given that the optimized Gaussians are flat, we can encode the information about their position and shape into a triangle soup proxy structure [23].

Suppose $\mathbf{m}$, $\mathbf{R}$, and $\mathbf{s}$ are, respectively the location of the center, the rotation matrix, and the scaling vector of a single Gaussian. A triangle $\mathbf{V}$ corresponding to this Gaussian is defined as an ordered set of its vertices $[\mathbf{v}_0, \mathbf{v}_1, \mathbf{v}_2]$, where $\mathbf{v}_0 = \mathbf{m}$, $\mathbf{v}_1 = s_1 \cdot \mathbf{r}_1$, and $\mathbf{v}_2 = s_2 \cdot \mathbf{r}_2$, with $\mathbf{r}_i$ being the ith column of the rotation matrix $\mathbf{R}$.

Associating each Gaussian with a single triangle results in a triangle soup. Because this process is reversible, given a triangle soup, we can recover the shape and location of each Gaussian. More specifically, given a new face $\mathbf{V}'$, the recovered position $\mathbf{m}'$ is $\mathbf{v}'_0$ and the columns $\mathbf{r}'_0$, $\mathbf{r}'_1$, and $\mathbf{r}'_2$ of the recovered rotation matrix are given by:

$$\mathbf{r}'_0 = \frac{(\mathbf{v}'_1 - \mathbf{v}'_0) \times (\mathbf{v}'_2 - \mathbf{v}'_0)}{\|(\mathbf{v}'_1 - \mathbf{v}'_0) \times (\mathbf{v}'_2 - \mathbf{v}'_0)\|} , \ \mathbf{r}'_1 = \frac{\mathbf{v}'_1 - \mathbf{v}'_0}{\|\mathbf{v}'_1 - \mathbf{v}'_0\|} ,$$

and $\mathbf{r}'_2$ is the orthonormal projection of $\mathbf{v}'_2 - \mathbf{v}'_0$ onto the plane spanned by $\mathbf{r}'_0$ and $\mathbf{r}'_1$. The corresponding scaling parameters are then $s_0 = \varepsilon$, $s_1 = \|\mathbf{v}'_1 - \mathbf{v}'_0\|$, and $s_2 = \langle \mathbf{v}'_2 - \mathbf{v}'_0, \mathbf{r}'_2 \rangle$. We refer the reader to [23] for more details.

To modify the appearance model optimized in the second stage, we first need to manually adjust the mesh extracted in the first stage, which we denote by $\mathcal{M}$. This can be easily achieved using any of a vast array of geometry sculpting tools, such as Blender. As a result, we obtain a modified mesh, denoted by $\mathcal{M}'$. This modification can be then propagated to the triangle soup proxy as follows.

Observe that there is a one-to-one correspondence between the triangles composing $\mathcal{M}$ and the triangles composing $\mathcal{M}'$. For each triangle $\mathbf{V}$ in the extracted triangle soup $\mathcal{T}$, we first find a triangle $\mathbf{W} \in \mathcal{M}$ such that the distance between the centers of the two is minimized.

Each face $\mathbf{W} = [\mathbf{w}_0, \mathbf{w}_1, \mathbf{w}_2]$ can be associated with an orthonormal basis $\mathbf{U}$, where the first two column vectors are given by

$$\mathbf{u}_0 = \frac{\mathbf{w}_1 - \mathbf{w}_0}{\|\mathbf{w}_1 - \mathbf{w}_0\|} , \ \mathbf{u}_1 = \frac{(\mathbf{w}_1 - \mathbf{w}_0) \times (\mathbf{w}_2 - \mathbf{w}_0)}{\|(\mathbf{w}_1 - \mathbf{w}_0) \times (\mathbf{w}_2 - \mathbf{w}_0)\|} ,$$

and the third one, $\mathbf{u}_2$, is the cross product of those two. Similarly, we associate the corresponding face $\mathbf{W}' \in \mathcal{M}'$ with an orthonormal basis $\mathbf{U}'$.

In this way, we obtain a linear transformation $\mathbf{T} = \mathbf{U}'\mathbf{U}^{-1}$ that transforms $\mathbf{W}$ into $\mathbf{W}'$ (notice that the bases are orthonormal, and hence $\mathbf{U}$ is invertible). Finally, we apply the associated transform $\mathbf{T}$ to each triangle $\mathbf{V} \in \mathcal{T}$, thus obtaining a modified triangle soup $\mathcal{T}'$. Formally, each new triangle is given by

$$\mathbf{V}' = \mathbf{T}(\mathbf{V} - \mathbf{w}_0) + \mathbf{w}'_0 ,$$

where we first subtract the reference vertex $\mathbf{w}_0$ to recenter the triangle vertices, and then translate the modified triangle by $\mathbf{w}'_0$ to position it in its new location. Note that the exact values of $\mathbf{T}$, $\mathbf{w}$ and $\mathbf{w}'$ depend on the triangle $\mathbf{V} \in \mathbf{T}$ being currently processed.

The updated triangles $\mathbf{V}' \in \mathcal{T}'$ are transformed into new locations and shapes of Gaussians using the procedure outlined above, while the rest of their parameters remain the same. An illustration of the modification process for a single proxy triangle is provided in Figure 4.

4. Experiments

Numerical results. We assess the qualitative performance of our method in the tasks of geometry reconstruction and novel-view synthesis. For geometry reconstruction, we utilize the DTU dataset, employing the Chamfer-L_1 distance metric to measure the surface quality. The DTU dataset provides 2D ground truth images with a resolution

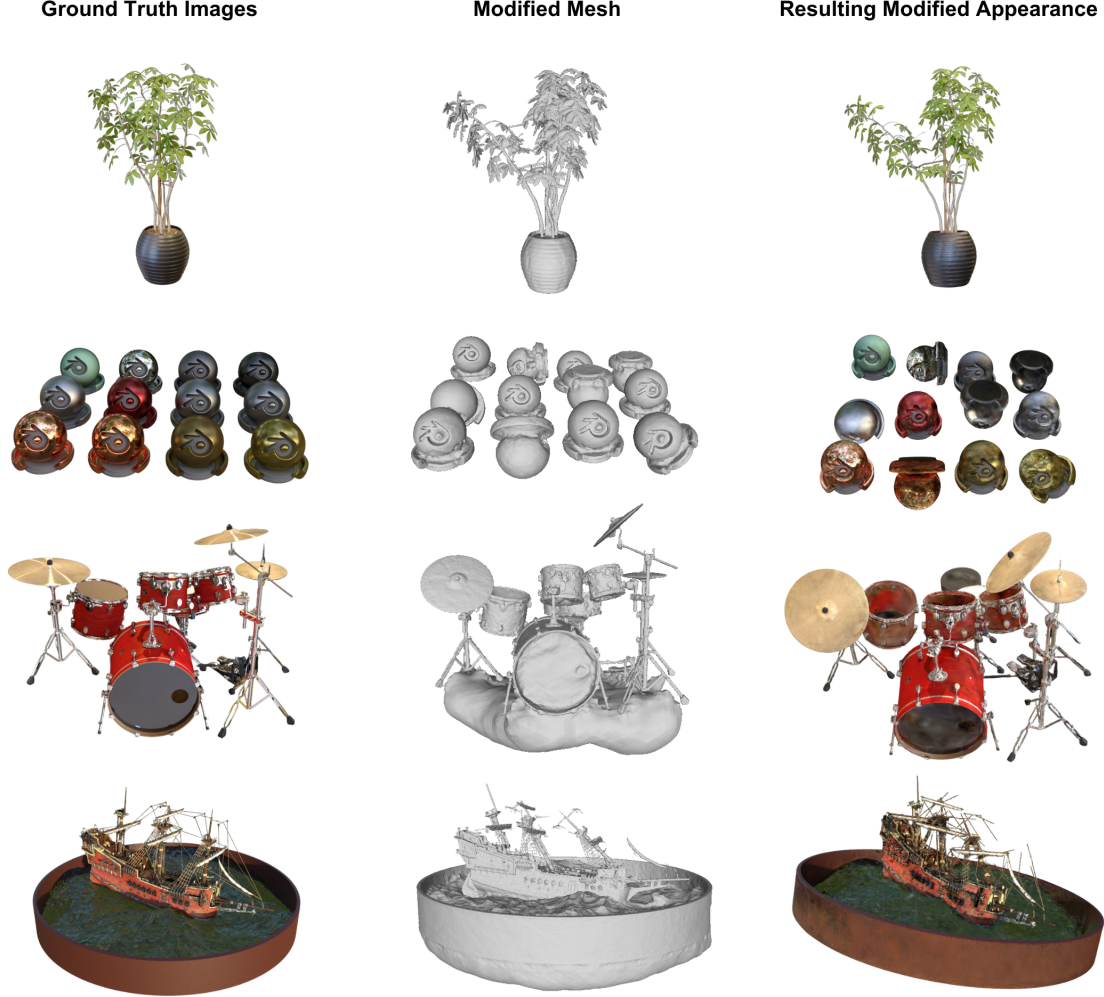| Ground Truth Images | Modified Mesh | Resulting Modified Appearance |

Figure 5. Example modifications produced with our method for scenes in the NeRF Synthetic dataset. First row: ficus with a repositioned branch. Second row: various rotations applied to objects in the materials scene. Third row: the drums scene with a displaced cymbal. Fourth: broken masts in the ship scene. These scenes have been edited in Blender using a combination of the translate, rotate, knife, bevel, and randomize tools.

of 1600×1200, along with associated camera poses, and features objects with various material properties. Depending on the selected scene, the dataset includes either 49 or 64 RGB images. We compare our approach against several established methods: NeuS [24], NeRF [12], VolSDF [26], Relightable 3D Gaussian (ReGS) [5], 3DGSR [11] and COLMAP [20].

Table 1 demonstrates that our method surpasses other state-of-the-art methods in terms of the surface reconstruction quality, as measured by the Chamfer-L_1 distance. We tested our method in two scenarios: images with and without masks. The values for the reference methods were calculated for images without masks. Regardless of whether we use a DTU dataset with masks or without masks, our method allows us to obtain meshes of very high quality.

For novel-view synthesis, we evaluate the PSNR on the NeRF Synthetic dataset, which consists of eight manually designed scenes. Each scene includes 100 training images with a resolution of 800×800.

Table 2 shows the novel view synthesis evaluation results. We compare our approach with NeRF [12], Instant NGP (Ins-NGP) [13], Mip-NeRF [1], 3DGSR [11], NeuS [24], NeRO [9], BakedSDF [27], and NeRF2Mesh [21].

Among the SDF-based models, our approach achieves the best results for the chair, drums, hotdog, lego and mic scenes. Across all models in the comparison, we achieve the highest PSNR value for the mic and hotdog scene and the highest average PSNR across all scenes.

Figure 6. Progression of a soft body simulation of a Ficus plant. Top row: changes in the object's geometry. Bottom row: corresponding modifications in appearance obtained using our method.

Scan ID	24	37	40	55	63	65	69	83	97	105	106	110	114	118	122	Avg
COLMAP	0.81	2.05	0.73	1.22	1.79	1.58	1.02	3.05	1.40	2.05	1.00	1.32	0.49	0.78	1.17	1.36
NeRF	1.90	1.60	1.85	0.58	2.28	1.27	1.47	1.67	2.05	1.07	0.88	2.53	1.06	1.15	0.96	1.49
NeuS	1.00	1.37	0.93	0.43	1.10	0.65	0.57	1.48	1.09	0.83	0.52	1.20	0.35	0.49	0.54	0.84
VolSDF	1.14	1.26	0.81	0.49	1.25	0.70	0.72	1.29	1.18	0.70	0.66	1.08	0.42	0.61	0.55	0.86
ReGS	1.21	1.00	1.10	0.87	1.03	1.51	1.51	1.06	1.63	0.97	1.36	1.21	0.94	1.38	1.26	1.20
3DGSR	0.68	0.84	0.70	0.39	1.16	0.87	0.77	1.48	1.26	0.87	0.69	0.80	0.42	0.64	0.60	0.81
Ours (w/ mask)	0.52	0.67	0.34	0.37	0.93	0.60	0.57	1.22	0.79	0.67	0.49	0.75	0.36	0.42	0.47	0.61
Ours (w/o mask)	0.52	0.75	0.41	0.37	0.90	0.66	0.59	1.37	1.08	0.85	0.46	0.98	0.33	0.49	0.50	0.68

Table 1. We evaluate the accuracy of surface reconstruction, with color-coded cells denoting the top-performing results with respect to Chamfer-L_1 distance. Our approach is compared to multiple state-of-the-art methods. It demonstrates superior performance over all competitors, achieving the lowest error.

Editing 3D objects   To illustrate the applicability of our approach, we conducted a series of adjustments on selected scenes, focusing on edits that mirror that of typical everyday environments, such as reorienting a branch of a plant. To modify the geometry, we used Blender, and then propagated these modifications to the appearance models using our method. The results are presented in Figure 5 and showcase a combination of the translate, rotate, knife, bevel, and randomize Blender tools applied to various scenes. Additionally, we showcase in Figure 7 that our method is capable of modifications directly on the triangle soup with arbitrary transforms such as non-linearly warping the ship scene.

Physics   We assessed the performance of our method in dynamic scenarios by running soft body simulations in Blender. These simulations allow objects to exhibit flexible movements. Using our method, we transferred the re-

sulting dynamics from the surface of the mesh to the object's appearance, as illustrated in Figure 6. While initially the dynamics are captured effectively, as the simulation progresses, an increasing number of artifacts becomes noticeable.

5. Conclusion

In this paper, we introduced a 3DGS-based method for geometry and appearance recovery from ground truth image data, which supports mesh-guided scene modification using a pretrained neural surface prior. Our method aims to maintain high visual fidelity in edits while providing flexibility during the editing process improving the workflow of computer graphics artists.

While this approach allows users to easily modify the recovered appearance by adjusting the underlying mesh geometry, it also faces limitations. First, the editing process is

	Chair	Drums	Ficus	Hotdog	Lego	Materials	Mic	Ship	Avg
NeRF	34.17	25.08	30.39	36.82	33.31	30.03	34.78	29.30	31.74
Ins-NGP	35.00	26.02	33.51	37.40	36.39	29.78	36.22	31.10	33.18
Mip-NeRF	35.14	25.48	33.29	37.48	35.70	30.71	36.51	30.41	33.09
3D-GS	35.36	26.15	34.87	37.72	35.78	30.00	35.36	30.80	33.32
NeuS	31.22	24.85	27.38	36.04	34.06	29.59	31.56	26.94	30.20
NeRO	28.74	24.88	28.38	32.13	25.66	24.85	28.64	26.55	27.48
BakedSDF	31.65	20.71	26.33	36.38	32.69	30.48	31.52	27.55	29.66
NeRF2Mesh	34.25	25.04	30.08	35.70	34.90	26.26	32.63	29.47	30.88
3DGSR	34.85	26.08	35.17	36.88	34.90	30.03	36.44	31.48	33.23
Ours	35.32	26.09	34.32	37.77	35.42	29.22	36.62	30.64	33.18

Table 2. Comparison of performance in novel view synthesis. All methods have been categorized as either SDF-based (top) no-SDF (bottom). In several scenes, our method achieves the highest PSNR score.
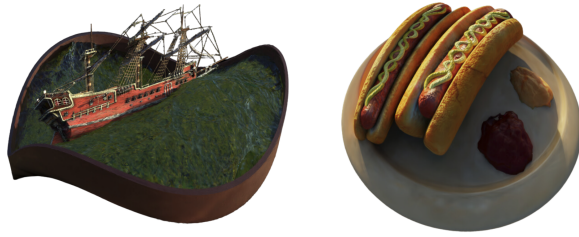

Figure 7. Our framework also allows to apply arbitrary, non-mesh-guided transforms to the recovered appearance by directly modifying the vertices of proxy triangles, similar to GaMeS [23].

highly dependent on the accuracy of the estimated mesh. Scenes with complex, fine-grained geometric details are challenging for surface extracting methods, consequently making precise mesh editing more difficult. Enhancing the resilience to input inaccuracies is a potential area for improvement. Furthermore, while certain mesh editing operations such as translation, scaling, shearing, rotation or other commonly available operations are well supported by our method, a mesh editing operation resulting in a different number of faces is not supported by our method.

Finally, editing operations such as translations may introduce appearance inconsistencies. An example, would be a shadow embedded in the recovered appearance of objects which would remain after a subcomponent of the reconstructed scene has been moved to a different location. In such cases relighting approaches would have to be used to remove such inconsistencies from the scene.

References

[1] Jonathan T. Barron, Ben Mildenhall, Matthew Tancik, Peter Hedman, Ricardo Martin-Brualla, and Pratul P. Srinivasan. Mip-nerf: A multiscale representation for anti-aliasing neural radiance fields. *ICCV*, 2021. 6

[2] Anpei Chen, Zexiang Xu, Andreas Geiger, Jingyi Yu, and Hao Su. Tensorf: Tensorial radiance fields, 2022. 1

[3] Hanlin Chen, Chen Li, and Gim Hee Lee. Neusg: Neural implicit surface reconstruction with 3d gaussian splatting guidance, 2023. 3, 4

[4] Robert A. Drebin, Loren Carpenter, and Pat Hanrahan. Volume rendering. In *Proceedings of the 15th Annual Conference on Computer Graphics and Interactive Techniques*, page 65–74, New York, NY, USA, 1988. Association for Computing Machinery. 2

[5] Jian Gao, Chun Gu, Youtian Lin, Hao Zhu, Xun Cao, Li Zhang, and Yao Yao. Relightable 3d gaussian: Real-time point cloud relighting with brdf decomposition and ray tracing. *arXiv:2311.16043*, 2023. 6

[6] M. Goesele, B. Curless, and S.M. Seitz. Multi-view stereo revisited. In *2006 IEEE Computer Society Conference on Computer Vision and Pattern Recognition (CVPR'06)*, pages 2402–2409, 2006. 2

[7] Antoine Guédon and Vincent Lepetit. Sugar: Surface-aligned gaussian splatting for efficient 3d mesh reconstruction and high-quality mesh rendering. In *Proceedings of the IEEE/CVF Conference on Computer Vision and Pattern Recognition*, pages 5354–5363, 2024. 2, 3

[8] Bernhard Kerbl, Georgios Kopanas, Thomas Leimkühler, and George Drettakis. 3d gaussian splatting for real-time radiance field rendering. *ACM Transactions on Graphics*, 42 (4), 2023. 1, 2, 4

[9] Yuan Liu, Peng Wang, Cheng Lin, Xiaoxiao Long, Jiepeng Wang, Lingjie Liu, Taku Komura, and Wenping Wang. Nero: Neural geometry and brdf reconstruction of reflective objects from multiview images. In *SIGGRAPH*, 2023. 6

[10] William E. Lorensen and Harvey E. Cline. Marching cubes: A high resolution 3d surface construction algorithm. In *Proceedings of the 14th Annual Conference on Computer Graphics and Interactive Techniques*, page 163–169, New York, NY, USA, 1987. Association for Computing Machinery. 2

[11] Xiaoyang Lyu, Yang-Tian Sun, Yi-Hua Huang, Xiuzhe Wu, Ziyi Yang, Yilun Chen, Jiangmiao Pang, and Xiaojuan Qi.

3dgsr: Implicit surface reconstruction with 3d gaussian splatting, 2024. 3, 4, 6

[12] Ben Mildenhall, Pratul P. Srinivasan, Matthew Tancik, Jonathan T. Barron, Ravi Ramamoorthi, and Ren Ng. Nerf: Representing scenes as neural radiance fields for view synthesis, 2020. 1, 2, 6

[13] Thomas Müller, Alex Evans, Christoph Schied, and Alexander Keller. Instant neural graphics primitives with a multiresolution hash encoding. *ACM Trans. Graph.*, 41(4):102:1–102:15, 2022. 6

[14] Thomas Müller, Alex Evans, Christoph Schied, and Alexander Keller. Instant neural graphics primitives with a multiresolution hash encoding. *ACM Transactions on Graphics*, 41 (4):1–15, 2022. 1, 2, 4

[15] Timothy S Newman and Hong Yi. A survey of the marching cubes algorithm. *Computers & Graphics*, 30(5):854–879, 2006. 2

[16] Onur Ozyesil, Vladislav Voroninski, Ronen Basri, and Amit Singer. A survey of structure from motion, 2017. 2

[17] Keunhong Park, Utkarsh Sinha, Jonathan T. Barron, Sofien Bouaziz, Dan B Goldman, Steven M. Seitz, and Ricardo Martin-Brualla. Nerfies: Deformable neural radiance fields, 2021. 3

[18] Albert Pumarola, Enric Corona, Gerard Pons-Moll, and Francesc Moreno-Noguer. D-nerf: Neural radiance fields for dynamic scenes, 2020. 3

[19] Radu Alexandru Rosu and Sven Behnke. Permutosdf: Fast multi-view reconstruction with implicit surfaces using permutohedral lattices, 2023. 2, 3, 4

[20] Johannes L. Schönberger and Jan-Michael Frahm. Structure-from-motion revisited. In *2016 IEEE Conference on Computer Vision and Pattern Recognition (CVPR)*, pages 4104–4113, 2016. 2, 4, 6

[21] Jiaxiang Tang, Hang Zhou, Xiaokang Chen, Tianshu Hu, Errui Ding, Jingdong Wang, and Gang Zeng. Delicate textured mesh recovery from nerf via adaptive surface refinement. *arXiv preprint arXiv:2303.02091*, 2022. 6

[22] Joanna Waczyńska, Piotr Borycki, Joanna Kaleta, Sławomir Tadeja, and Przemysław Spurek. D-miso: Editing dynamic 3d scenes using multi-gaussians soup. *arXiv preprint arXiv:2405.14276*, 2024. 3

[23] Joanna Waczyńska, Piotr Borycki, Sławomir Tadeja, Jacek Tabor, and Przemysław Spurek. Games: Mesh-based adapting and modification of gaussian splatting. *arXiv preprint arXiv:2402.01459*, 2024. 2, 3, 4, 5, 8

[24] Peng Wang, Lingjie Liu, Yuan Liu, Christian Theobalt, Taku Komura, and Wenping Wang. Neus: Learning neural implicit surfaces by volume rendering for multi-view reconstruction, 2023. 2, 3, 6

[25] Yiming Wang, Qin Han, Marc Habermann, Kostas Daniilidis, Christian Theobalt, and Lingjie Liu. Neus2: Fast learning of neural implicit surfaces for multi-view reconstruction, 2023. 2

[26] Lior Yariv, Jiatao Gu, Yoni Kasten, and Yaron Lipman. Volume rendering of neural implicit surfaces. In *Thirty-Fifth Conference on Neural Information Processing Systems*, 2021. 6

[27] Lior Yariv, Peter Hedman, Christian Reiser, Dor Verbin, Pratul P. Srinivasan, Richard Szeliski, Jonathan T. Barron, and Ben Mildenhall. Bakedsdf: Meshing neural sdfs for real-time view synthesis, 2023. 2, 3, 6

[28] Alex Yu, Sara Fridovich-Keil, Matthew Tancik, Qinhong Chen, Benjamin Recht, and Angjoo Kanazawa. Plenoxels: Radiance fields without neural networks, 2021. 1